

Synthesis, characterisation and theoretical study of ruthenium 4,4'-bi-1,2,3-triazolyl complexes: fundamental switching of the nature of S₁ and T₁ states from MLCT to MC[†]

Christine E. Welby,^a Stev Grkinic,^a Adam Zahid,^a Baljinder S. Uppal,^a Elizabeth A. Gibson,^b Craig R. Rice^a and Paul I. P. Elliott^{*a}

Received 2nd March 2012, Accepted 27th April 2012

DOI: 10.1039/c2dt30510k

The series of complexes [Ru(bpy)_{3-n}(btz)_n][PF₆]₂ (bpy = 2,2'-bipyridyl, btz = 1,1'-dibenzyl-4,4'-bi-1,2,3-triazolyl, **2** *n* = 1, **3** *n* = 2, **4** *n* = 3) have been prepared and characterised, and the photophysical and electronic effects imparted by the btz ligand were investigated. Complexes **2** and **3** exhibit MLCT absorption bands at 425 and 446 nm respectively showing a progressive blue-shift in the absorption on increasing the btz ligand content when compared to [Ru(bpy)₃][Cl]₂ (**1**). Complex **4** exhibits a heavily blue-shifted absorption spectrum with respect to those of **1–3**, indicating that the LUMO of the latter are bpy-centred with little or no btz contribution whereas that of **4** is necessarily btz-centred. DFT calculations on analogous complexes **1'–4'** (in which the benzyl substituents are replaced by methyl) show that the HOMO–LUMO gap increases by 0.3 eV from **1'–3'** through destabilisation of the LUMO with respect to the HOMO. The HOMO–LUMO gap of **4'** increases by 0.98 eV compared to that of **3'** due to significant destabilisation of the LUMO. Examination of TDDFT data show that the S₁ states of **1'–3'** are ¹MLCT in character whereas that of **4'** is ¹MC. The optimisation of the T₁ state of **4'** leads to the elongation of two mutually *trans* Ru–N bonds to yield [Ru(κ²-btz)(κ¹-btz)₂]²⁺, confirming the ³MC character. Thus, replacement of bpy by btz leads to a fundamental change in the ordering of excited states such that the nature of the lowest energy excited state changes from MLCT in nature to MC.

Introduction

The Huisgen–Sharpless copper catalysed alkyne–azide 1,3-dipolar cycloaddition (CuAAC) to form 1,4-disubstituted-1,2,3-triazoles¹ has in the past decade become an invaluable synthetic tool in organic synthesis,² materials and polymer science^{3–7} and in the derivatisation of biological macromolecules.^{8,9} The reaction benefits from high efficiency, selectivity and broad functional group tolerance with a minimal work-up often required for product isolation.

Recently the reaction has begun to attract significant attention for its application in the design of new hybrid ligand systems for transition metal complexes.^{10–39} Ligand systems, ubiquitous in

coordination chemistry due to the photophysical properties of their resultant complexes, include 2,2-bipyridyl (bpy) and 2,2':6',2''-terpyridyl (tpy). Several CuAAC-derived analogues of these ligands are now known. The complexes [Ru(tpy)(dtzpy)]²⁺ and [Ru(dtzpy)₂]²⁺ (dtzpy = 2,6-di(1,2,3-triazol-4-yl)pyridine)³² have been prepared, for example. These show blue-shifting of the ¹MLCT bands on replacement of tpy by dtzpy which is expected as a result of the truncation of the ligand π-system, resulting in the destabilization of the LUMO relative to the HOMO in these complexes.

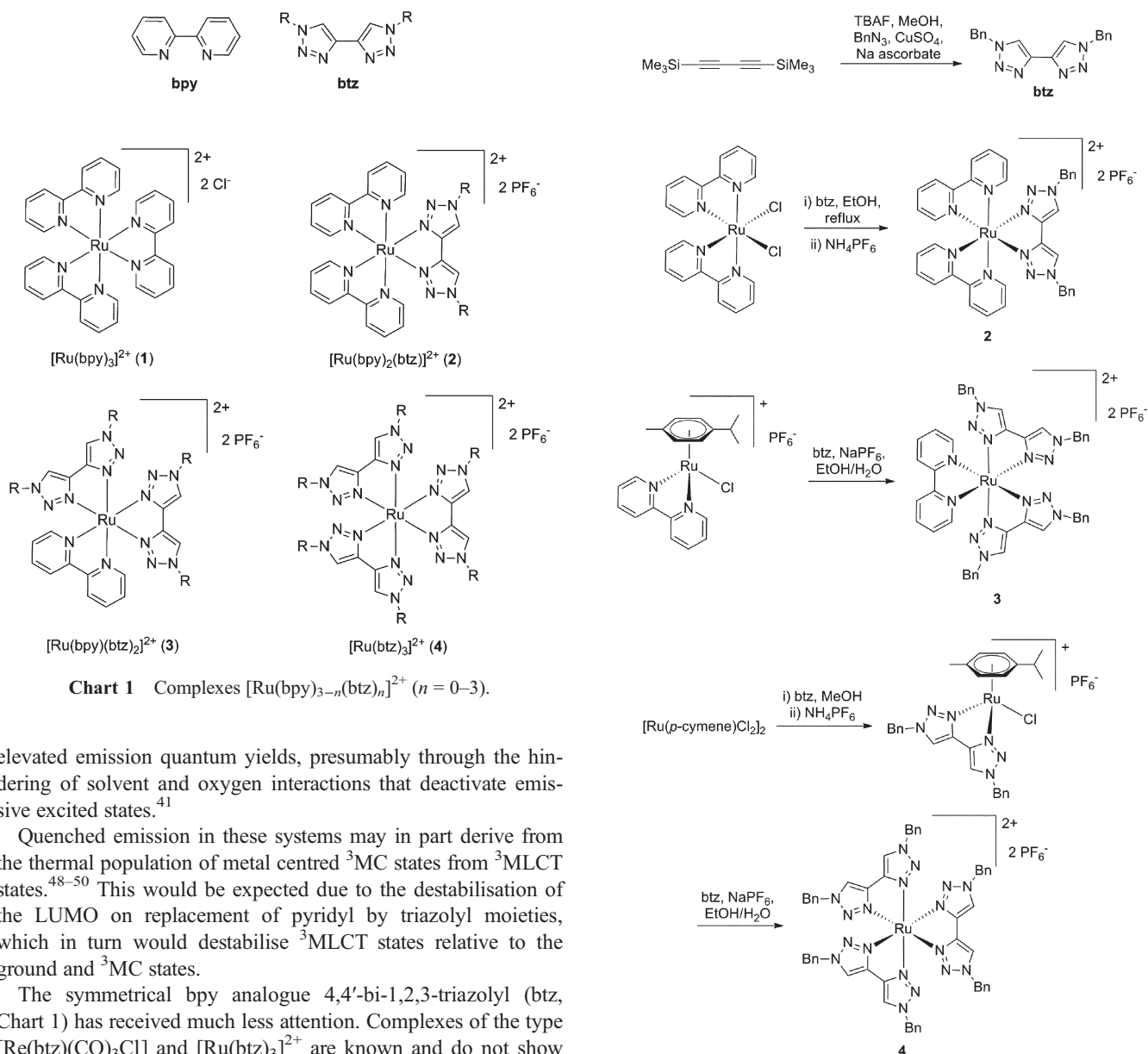
Complexes of the bidentate bpy analogue 4-(pyrid-2-yl)-1,2,3-triazole (pytz) have been prepared with rhenium,⁴⁰ iridium^{41–44} and ruthenium.^{45,46} Complexes of the form [Ru(dcb)(pytz)(NCS)₂] (dcb = 2,2'-bipyridyl-4,4'-dicarboxylic acid) have been shown to be promising candidates for dye-sensitized solar cell applications.⁴⁷ These complexes also display blue-shifted absorption spectra relative to those of their bpy analogues and also exhibit blue-shifted and often highly quenched emission spectra. The complex [Re(pytz)(CO)₃Cl] is however observed to have an elongated luminescent lifetime and a greater emission quantum yield compared to its bpy analogue.⁴⁰ Cyclometallated Ir(III) complexes with pytz ancillary ligands also show attractive photophysical properties. Incorporation of a cyclodextrin into the 1-position of the pytz ligand has been shown to promote

^aDepartment of Chemical & Biological Sciences, University of Huddersfield, Queensgate, Huddersfield HD1 3DH, UK.

E-mail: p.i.elliott@hud.ac.uk; Tel: +44 (0)1484 472320

^bSchool of Chemistry, University of Nottingham, University Park, Nottingham NG7 2RD, UK

[†]Electronic supplementary information (ESI) available: NMR spectra of complexes, graphical plots of molecular orbitals for complexes from DFT calculations, *x,y,z* coordinate files for optimised geometries of singlet ground and triplet excited states for complexes and crystallographic information for complex **2**. CCDC reference number 866315. For ESI and crystallographic data in CIF or other electronic format see DOI: 10.1039/c2dt30510k



elevated emission quantum yields, presumably through the hindering of solvent and oxygen interactions that deactivate emissive excited states.⁴¹

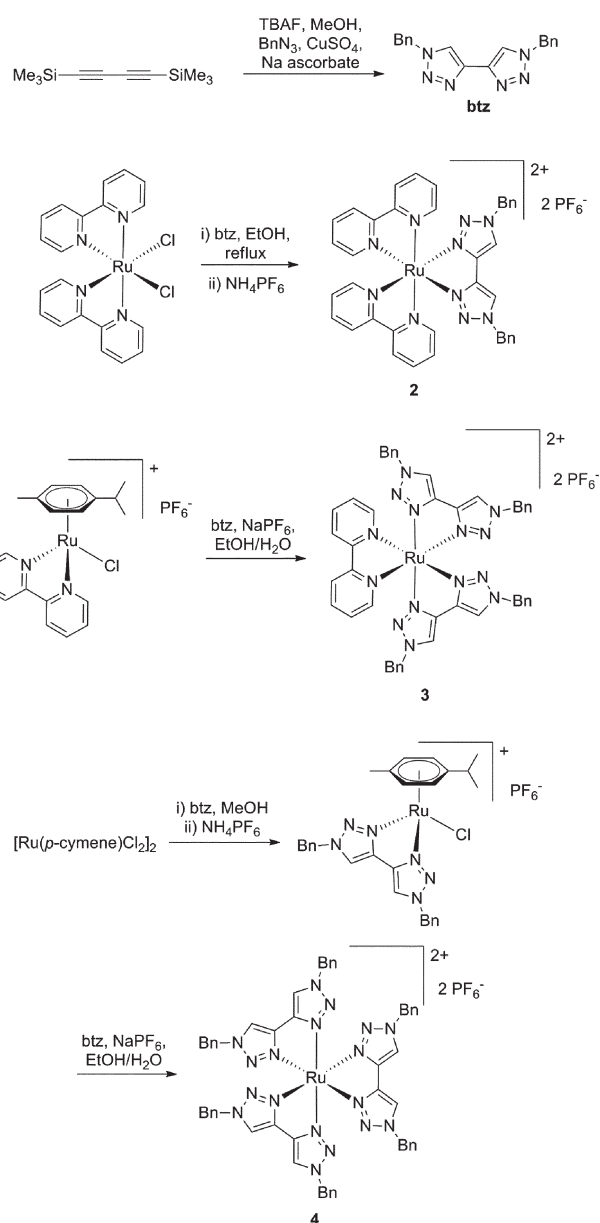
Quenched emission in these systems may in part derive from the thermal population of metal centred ^3MC states from $^3\text{MLCT}$ states.⁴⁸⁻⁵⁰ This would be expected due to the destabilisation of the LUMO on replacement of pyridyl by triazolyl moieties, which in turn would destabilise $^3\text{MLCT}$ states relative to the ground and ^3MC states.

The symmetrical bpy analogue 4,4'-bi-1,2,3-triazolyl (btz, Chart 1) has received much less attention. Complexes of the type $[\text{Re}(\text{btz})(\text{CO})_3\text{Cl}]$ and $[\text{Ru}(\text{btz})_3]^{2+}$ are known and do not show any luminescent emission at room temperature.^{51,52} Mattiuzzi *et al.* have recently conducted investigations of the spectroscopic and electrochemical properties of complexes of the form $[\text{Ru}(\text{tap})_2(\text{btz})]^{2+}$ and $[\text{Ru}(\text{tap})_2(\text{pytz})]^{2+}$ (tap = 1,4,5,8-tetraazaphenanthrene) and have shown that these complexes should behave as highly photo-oxidising agents under illumination.⁵³

In order to gain a deeper understanding of the photophysical and electronic properties imparted by this ligand, we report here results from experimental and theoretical investigations of the series of complexes $[\text{Ru}(\text{bpy})_{3-n}(\text{btz})_n]^{2+}$ ($n = 0-3$, Chart 1).

Results and discussion

The benzyl substituted btz ligand 1,1'-dibenzyl-4,4'-bi-1,2,3-triazole was prepared in good yield in a one-pot procedure from 1,4-bis(trimethylsilyl)buta-1,3-diyne and benzyl azide in the presence of tetrabutyl ammonium fluoride, copper sulfate and sodium ascorbate (Scheme 1). The ^1H NMR spectrum in d_3 -



MeCN of the product is in agreement with that previously reported⁵² and exhibits a singlet for the triazole ring protons at δ 8.17, a singlet for the methylene protons at δ 5.62 and a multiplet for the phenyl ring protons at δ 7.36-7.41.

$[\text{Ru}(\text{bpy})_2\text{Cl}_2]$ was combined with an equivalent of the btz ligand in ethanol and heated to reflux. The product $[\text{Ru}(\text{bpy})_2(\text{btz})][\text{PF}_6]_2$ (**2**) was then isolated on addition of ammonium hexafluorophosphate as an orange powder. Upon coordination to the metal, the resonance for the triazole protons in the ^1H NMR spectrum shifts to a slightly lower field and appears at δ 8.37. The methylene protons result in a pair of geminal doublets at δ 5.50 and 5.55, which show an AB pattern with significant roofing ($^2J_{\text{HH}} = 14.9$ Hz). Seven signals are observed for the bpy ligands with the resonances of the bpy H3 and H3' protons being coincident. This reflects the asymmetry

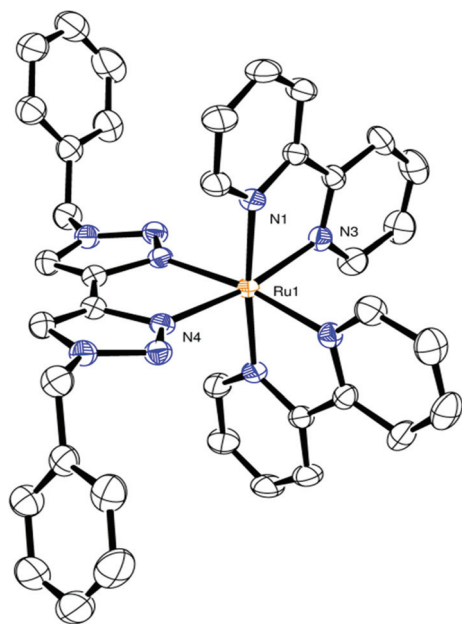


Fig. 1 ORTEP plot of the $[\text{Ru}(\text{bpy})_2(\text{btz})]^{2+}$ cation (the counter ions, hydrogen atoms and solvent are removed for clarity).

within the bpy ligands where one pyridyl ring of each bpy is *trans* to btz whilst the other rings of the bpy ligands are mutually *trans* to each other.

Crystals of X-ray diffraction quality were grown from an acetonitrile solution with slow vapour diffusion of diethyl ether. The complex crystallizes as the solvate $[\text{Ru}(\text{bpy})_2(\text{btz})][\text{PF}_6]_2 \cdot 2\text{MeCN}$ in the Pbcn space group. An ORTEP plot of the structure of the cation is shown in Fig. 1, whilst Table 1 contains selected bond lengths and angles. The cation that exhibits a distorted octahedral geometry lies on a C_2 axis such that only half of it (one bpy ligand and half of the btz ligand) is crystallographically unique. The Ru–N(btz) bond lengths are comparable at 2.0593(18) Å to the Ru–N(bpy) ligands (2.0529(19) Å *trans* to btz and 2.0630(19) Å *cis* to btz). These bond distances are in the range quoted for the Ru–N bond lengths of the structure of $[\text{Ru}(\text{btz})_3]\text{Cl}_2$ reported by Monkowius *et al.* (2.05(3) Å, although the authors noted the low quality of their data in their report of this structure) and are similar to those reported for $[\text{Ru}(\text{bpy})_3]^{2+}$ (2.056(2) Å).⁵² The btz bite angle of 77.68(10)° is also similar to those observed for the homoleptic complex $[\text{Ru}(\text{btz})_3]\text{Cl}_2$ (77.1(12), 77.9(11) and 74.9(12)°). The most notable feature in the structure is a significant twist in between the planes of the triazole rings characterised by an N–C–C–N torsion angle about the inter-ring C–C bond of 11.91°. However, the DFT optimised geometry of the cation (*vide infra*) with a methyl analogue of the btz ligand does not show a comparable twist (only 2.3°), nor does the reported structure of $[\text{Ru}(\text{btz})_3]\text{Cl}_2$.⁵² This twisting may therefore be due to the crystal packing effects necessary to accommodate the benzyl substituents or as the result of intermolecular π – π stacking type interactions in the solid state. Indeed, the btz phenyl rings lie only ~3.4–3.5 Å away from a bpy ligand of a neighbouring cation.

The complex $[\text{Ru}(\text{bpy})(\text{btz})_2][\text{PF}_6]_2$ (**3**) was prepared from $[\text{Ru}(p\text{-cymene})(\text{bpy})\text{Cl}]\text{PF}_6$ by reaction with two equivalents of the btz ligand and NaPF_6 in 3 : 1 ethanol–water under reflux. On

Table 1 Selected bond lengths (Å) and angles (°) for $[\text{Ru}(\text{bpy})_2(\text{btz})][\text{PF}_6]_2 \cdot 2\text{MeCN}$

Ru1–N1	2.0630(19)	N1–Ru1–N3	78.88(8)
Ru1–N3	2.0529(19)	N1–Ru1–N4	93.58(7)
Ru1–N4	2.0593(18)	N4–Ru1–N3	170.01(7)
N4–Ru1–N4	77.68(10)	N1–Ru1–N1	174.26(10)

cooling, **3** precipitated as an orange–yellow microcrystalline powder which was purified by recrystallization from dichloromethane–diethyl ether. The ^1H NMR spectrum of **3** shows two resonances for the btz ligand triazole ring protons at δ 8.30 and 8.31 consistent with the asymmetric coordination environment where one triazole ring of each btz ligand is *trans* to bpy whilst the others are mutually *trans* to each other. The methylene protons of the btz ligand similarly give rise to two signals at δ 5.49 and 5.53. The first of these signals initially appears to be a broad singlet. On closer examination this shows evidence of an AB pattern, as for the methylene signal for **2**, as a pair of doublets ($J_{\text{HH}} = 15$ Hz). The inner lines are almost coincident and the outer lines of each doublet are very small.

The homoleptic complex $[\text{Ru}(\text{btz})_3][\text{PF}_6]_2$ (**4**) was prepared by an analogous route to that of **3** using the precursor complex $[\text{Ru}(p\text{-cymene})(\text{btz})\text{Cl}]\text{PF}_6$. Firstly, $[\text{Ru}(p\text{-cymene})\text{Cl}_2]_2$ was stirred in methanol with an equivalent of btz for 2 hours after which time excess NH_4PF_6 was added and the volume reduced to precipitate $[\text{Ru}(p\text{-cymene})(\text{btz})\text{Cl}]\text{PF}_6$. The ^1H NMR spectrum of the complex in d_3 -MeCN exhibits the expected pair of doublet resonances at δ 5.64 and 5.85 characteristic of the aryl ring protons of the cymene ligand. These straddle an AB pattern of doublets (δ 5.70 and 5.76, $^2J_{\text{HH}} = 14.9$ Hz) that show significant roofing and correspond to the *endo* and *exo* methylene protons of the btz benzyl substituents. The resonance for the triazole ring protons appears as a singlet at δ 8.27 and is marginally shifted to a lower field by 0.10 ppm relative to that of the free ligand in the same solvent.

The $[\text{Ru}(p\text{-cymene})(\text{btz})\text{Cl}]\text{PF}_6$ complex was then heated to reflux in 3 : 1 ethanol–water with two further equivalents of btz and NaPF_6 to yield **4**. The complex exhibits a very simple ^1H NMR spectrum with a singlet resonance for all six triazole ring protons at δ 8.34 and a multiplet for the phenyl groups over the range δ 7.11 to 7.13. The resonance for the methylene protons appears as a singlet at δ 5.52 rather than the geminal pattern observed for **2** and **3**.

UV-visible absorption spectra were recorded in acetonitrile for all the complexes and are shown in Fig. 2. Spectroscopic data for all the complexes are presented in Table 2. The spectra for complexes **1–3** all show an intense absorption band at approximately 290 nm, assigned to bpy-centred $\pi \rightarrow \pi^*$ excitation. For complexes **2** and **3** this band exhibits a shoulder at longer wavelengths (*vide infra*).

Each of these complexes also exhibits a broad band between 400–500 nm, assigned to $^1\text{MLCT}$ -based transitions. On replacement of bpy by btz these MLCT bands are observed to a blue-shift appearing at 446 nm for **2** and 425 nm for **3**, compared to 455 nm for **1**. This is consistent with the expectation that replacement of bpy with btz will destabilise the LUMO relative to the HOMO, resulting in a larger HOMO–LUMO gap.

On replacement of the final bpy ligand to give **4**, the absorption profile is observed to be dramatically blue-shifted relative to

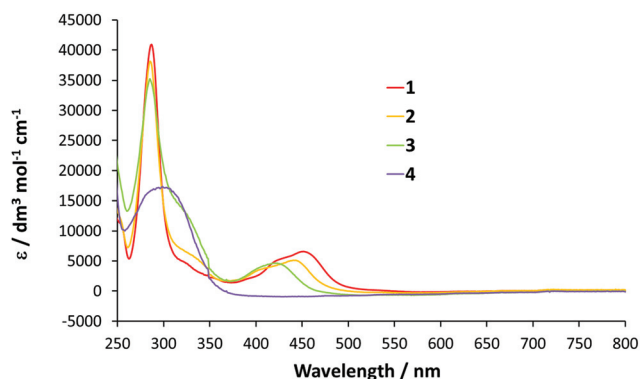


Fig. 2 UV-vis absorption spectra for complexes 1–4 in acetonitrile.

Table 2 UV-vis absorption and luminescence data for complexes 1–4 in acetonitrile

Complex	$\lambda^{\text{abs}}/\text{nm}$	RT $\lambda_{\text{max}}^{\text{em}}/\text{nm}$	77 K $\lambda^{\text{em}}/\text{nm}$
[Ru(bpy) ₃]Cl ₂ (1)	288, 455	610 ^a	
[Ru(bpy) ₂ (btz)][PF ₆] ₂ (2)	287, 446	~590 ^{a,b}	544, 585 ^c
[Ru(bpy)(btz) ₂][PF ₆] ₂ (3)	286, 425		565, 610 ^c
[Ru(btz) ₃][PF ₆] ₂ (4)	303		

^a Not corrected for detector response. ^b CH₂Cl₂. ^c 4 : 1 EtOH–MeOH glass.

those of 1–3 such that the complex has very little absorption at wavelengths longer than 370 nm. Indeed, compared to the red, orange and yellow solutions of 1, 2 and 3 respectively, the solutions of 4 are almost colourless to the eye. The spectrum contains a broad band centred at about 300 nm which we assign to ¹MLCT excitations.⁵² We therefore also tentatively assign the shoulders at ~300 nm in the spectra of 2 and 3 as arising from btz-centred ¹MLCT transitions.

The observations of the changes in the absorption spectra across the series lead us to conclude that the contribution from the btz ligands to the LUMO in 2 and 3 is very small and that these orbitals are therefore delocalised, primarily over the remaining bpy ligands. The large blue-shift in the absorption observed for 4 is therefore the result of the mandated change in localisation of the LUMO from a bpy ligand to the btz ligands. We surmise that the LUMO of the isolated btz is significantly destabilised with respect to that of bpy.

Of the btz-containing complexes only 2 shows observable, albeit very weak, luminescent emission at room temperature in an aerated solution. The emission spectrum of 2 is shown in Fig. 3a along with the trace for 1 for comparison (the spectra were not corrected for detector response). The emission profile is blue-shifted relative to that of 1 (610 nm), as expected from the blue-shift in the MLCT absorption band, with λ_{max} appearing at approximately 590 nm. Whilst it is too weak to obtain reliable lifetime measurements, the emission band is assigned as arising from a ³MLCT state.

The largely quenched room temperature emission observed for 2 and the lack of emission for 3 and 4 are proposed to be at least in part due to the thermal population of non-emissive ³MC states from elevated ³MLCT states, as mentioned above. The emission

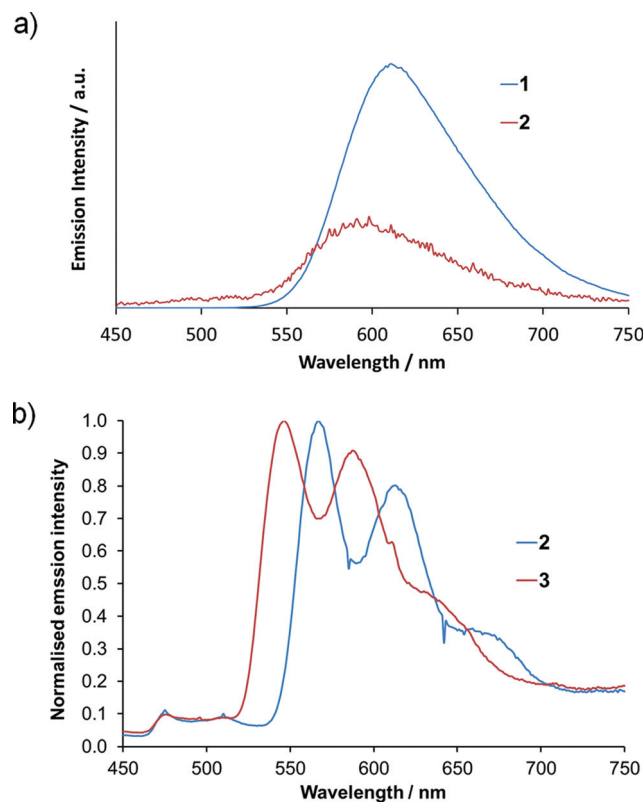


Fig. 3 (a) Emission spectra for complexes 1 (in MeCN) and 2 (in CH₂Cl₂, vertical scale magnified $\times 200$ with respect to that of 1), (b) normalised emission spectra for complexes 2 and 3 in 4 : 1 EtOH–MeOH glass at 77 K.

spectra of complexes 2–4 were recorded at 77 K (Fig. 3b) and structured emission bands are observed for 2 (544 & 585 nm) and 3 (565 & 610 nm), consistent with this proposal. No emission is observed for 4 however. The 77 K emission spectrum for 2 undergoes the expected rigidochromic blue-shift relative to that recorded at room temperature.

All the complexes were analysed by cyclic and pulsed voltammetry in order to obtain the first oxidation and reduction potentials to probe the effect of the btz ligand on the energies of the HOMO and LUMO for complexes 2–4. Complexes 2–4 show reversible Ru(II)–Ru(III) redox couples at 0.95, 0.98 and 1.01 V (vs. Fc–Fc⁺), respectively. Complex 2 exhibits a reversible reduction centred at –1.22 V assigned to a bpy-centred reduction. Reductions also seem to occur for 3 and 4, but the samples appear to undergo some degradation at these negative potentials. Due to this degradation, our electrochemical measurements are not particularly informative with regard to the frontier orbital make up of these complexes and are not discussed further.

The complexes described here were therefore additionally studied by density functional theory (DFT) methods to further evaluate the electronic and spectroscopic effects of increasing the btz ligand content. The singlet ground state geometries of all four complexes [Ru(bpy)_{3–n}(btz)_n]²⁺ (1'–4') were optimized in the gas phase at the B3LYP level of theory using the Stuttgart–Dresden small core potential for ruthenium and 6-311G* basis sets for all other atoms. To limit the computational expense, the

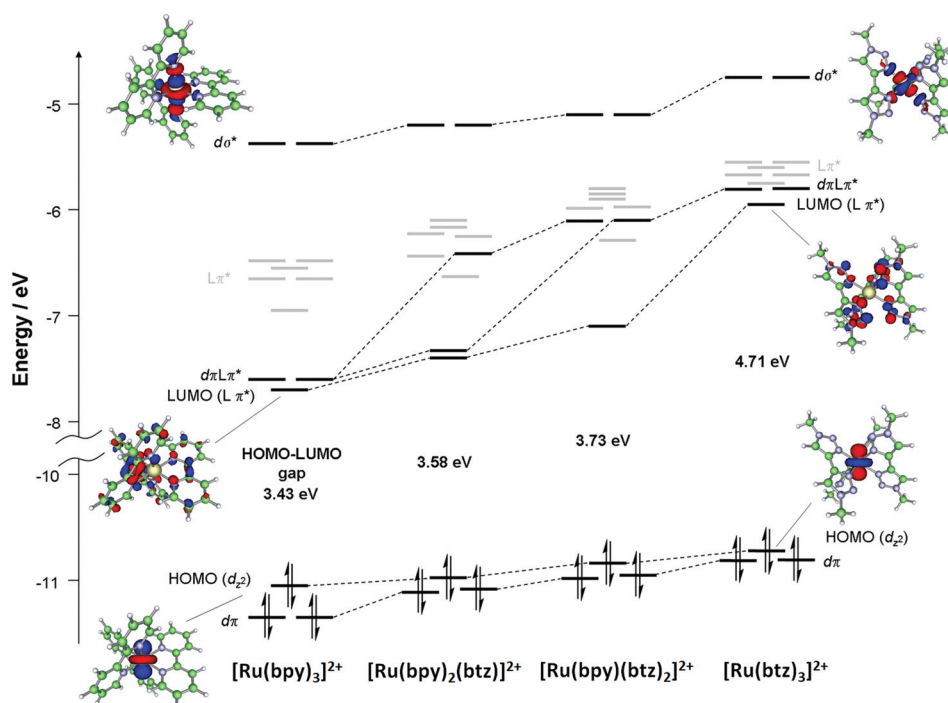


Fig. 4 Energy level diagram for the molecular orbitals for complexes $[\text{Ru}(\text{bpy})_{3-n}(\text{btz})_n]^{2+}$ with representative graphical plots of HOMO, LUMO and $d\sigma^*$ orbitals shown (principle d-orbital interactions and ligand centred LUMOs are in black, intervening ligand orbitals are in grey).

benzyl side chains of the btz ligands were simplified to methyl. The optimized geometries of complexes **1'**–**4'** are depicted in the ESI.† All the complexes adopt distorted octahedral geometries. In the heteroleptic complexes **2'** and **3'**, the average Ru–N(btz) bond lengths of 2.127 and 2.137 Å, respectively, are elongated relative to the corresponding Ru–N(bpy) bond lengths (2.104 and 2.100 Å, respectively). These calculated bond lengths for **2'** are slightly elongated relative to the crystallographic data for **2** by *ca.* 0.07 Å for btz and *ca.* 0.08 Å for bpy. The average Ru–N bond length for the homoleptic btz complex, **4'**, is shorter than those for **2'** and **3'** at 2.100 Å, but again elongated relative to the reported crystallographic structure for $[\text{Ru}(\text{btz})_3]\text{Cl}_2$ by approximately 0.05 Å.⁵²

The energies and plots of the principle molecular orbitals of interest in complexes **1'**–**4'** were calculated for the optimized ground state geometries. Fig. 4 shows a simplified molecular orbital energy level diagram for the series of complexes. The HOMO in all cases is composed primarily of the metal $4d_{z^2}$ orbital, whereas the LUMOs are composed primarily of ligand-centred π^* orbitals. The HOMO – 1 and HOMO – 2 orbitals for all the complexes are metal d-orbitals. In the case of complexes **1'** and **2'** the LUMO is spread equally over the bpy ligands, and in complex **3'** resides on the sole bpy ligand. In complex **4'** after the replacement of the third bpy ligand, the LUMO is spread equally across the three btz ligands.

Sequential replacement of bpy by btz leads to an overall destabilization of the orbital energies across the series with the HOMO increasing in energy by 0.48 eV. This is the opposite trend to that suggested by CV data, but it must be noted that these calculations are carried out in the gas phase and therefore in the absence of solvent interactions. Fletcher *et al.* also noted that the oxidation potential of $[\text{Ru}(\text{btz})_3]^{2+}$ -type complexes

showed a dependence on the nature of the btz ligand substituents.⁵¹ The addition of the first and second btz ligands in complexes **2'** and **3'** leads to greater destabilization of the LUMO relative to that of the HOMO such that the HOMO–LUMO gap increases by 0.3 eV on going from **1'** to **3'** from 3.43 to 3.73 eV. The replacement of the third bpy ligand by btz in complex **4'** results in a dramatic destabilization of the LUMO compared to that of **3'** and an increase in the magnitude of the HOMO–LUMO gap by 0.98 eV to 4.71 eV. Consistent with this, the LUMO for the free btz ligand fragment (derived by excision and optimisation of a btz ligand from the geometry of **4'**) lies 1.02 eV higher in energy than the LUMO of free bpy (similarly derived from the geometry of **1'**). From our calculations, the degenerate LUMO + 1 and LUMO + 2 orbitals for **1'** are $d\pi L\pi^*$ in character, as expected, and lie 0.1 eV above the LUMO. For **2'**, the comparable orbitals are LUMO + 1 and LUMO + 4 and are separated by 0.95 eV, straddling two intervening largely bpy π^* -based orbitals. Here, LUMO + 1 has a largely bpy character whereas LUMO + 4 has a btz character. For **3'**, the $d\pi L\pi^*$ orbitals are both significantly elevated with respect to the LUMO (0.96 eV higher in energy) and appear as LUMO + 2 and LUMO + 3, exhibiting significant btz character. For **4'**, the analogous orbitals are again LUMO + 1 and LUMO + 2, and now lie only 0.16 eV above the LUMO due to the dramatic destabilisation of the latter on replacement of the final bpy ligand by btz.

For all four complexes in the series, the $d\sigma^*$ anti-bonding orbitals are LUMO + 9 and LUMO + 10. For complexes **1'**–**3'** these orbitals lie between 2.32 to 1.98 eV above the LUMO, but for **4'** this separation is reduced to only 1.19 eV. This could therefore allow for dramatically destabilised MLCT states in **4** that would be in close proximity to metal-centred states and thus provide thermally accessible routes to non-radiative deactivation.

Table 3 TDDFT calculated energies, wavelengths and principle compositions of selected excitation transitions for complexes **1'**–**4'**

Complex	Excited state	Energy/eV (oscillator strength)	Wavelength/nm	Composition	
[Ru(bpy) ₃] ²⁺ (1')	S ₁	2.61 (0.00013)	476	HOMO → LUMO, HOMO → LUMO + 1, HOMO → LUMO + 2	MLCT
	S ₇	2.98 (0.102)	416	HOMO – 1 → LUMO, HOMO – 2 → LUMO	MLCT
	S ₁₉	3.88 (0.0259)	319	HOMO → LUMO + 7	MLCT
	S ₂₄	4.00 (0.0551)	310	HOMO – 1 → LUMO + 6, HOMO – 1 → LUMO + 4	MLCT
[Ru(bpy) ₂ (btz)] ²⁺ (2')	S ₁	2.72 (0.00099)	456	HOMO → LUMO	MLCT(bpy)
	S ₅	3.05 (0.114)	406	HOMO – 2 → LUMO, HOMO – 1 → LUMO + 1	MLCT(bpy)
	S ₆	3.18 (0.0406)	389	HOMO – 2 → LUMO + 1	MLCT(bpy)
	S ₁₉	4.00 (0.0682)	310	HOMO – 1 → LUMO + 3, HOMO → LUMO + 5	MLCT(bpy)
	S ₂₄	4.13 (0.0293)	300	HOMO – 1 → LUMO + 5	MLCT(bpy&btz)
	S ₂₅	4.13 (0.0348)	300	HOMO → LUMO + 5, HOMO → LUMO + 7	MLCT(bpy&btz)
[Ru(bpy)(btz) ₂] ²⁺ (3')	S ₁	2.85 (0.00062)	434	HOMO → LUMO	MLCT(bpy)
	S ₃	3.22 (0.0847)	386	HOMO – 2 → LUMO	MLCT(bpy)
	S ₁₂	3.95 (0.0504)	314	HOMO – 1 → LUMO + 1, HOMO – 2 → LUMO + 2	MLCT(bpy&btz)
	S ₁₃	3.70 (0.0400)	312	HOMO – 1 → LUMO + 2, HOMO → LUMO + 7	MLCT(btz)
	S ₁₈	4.16 (0.0819)	298	HOMO → LUMO + 7, HOMO – 2 → LUMO + 1, HOMO – 1 → LUMO + 2	MLCT(btz)
	[Ru(btz) ₃] ²⁺ (4')	S ₁	3.65 (0.00006)	340	HOMO → LUMO + 9
S ₁₀		4.08 (0.0697)	304	HOMO – 2 → LUMO	MLCT
S ₁₁		4.09 (0.0761)	303	HOMO – 2 → LUMO + 1, HOMO – 1 → LUMO	MLCT
S ₂₁		4.38 (0.123)	283	HOMO – 2 → LUMO + 6, HOMO → LUMO + 9	MLCT/MC

Time-dependent DFT (TDDFT) calculations were performed on the optimized geometries of the singlet ground states for each complex to determine the vertical excitation energies and their associated oscillator strengths (selected major transitions are listed in Table 3). The resultant calculated absorption spectra for **1'**–**4'** are presented in Fig. 5 with the experimentally observed spectra for **1**–**4** overlaid. Consistent with the trend of the increasing HOMO–LUMO gap and the spectroscopic data for complexes **1**–**4**, a visual analysis of the positions of the major vertical excitations show that the absorptions shift towards shorter wavelengths on replacement of bpy with btz when going from complex **1'** to **3'**. On addition of the third btz ligand in complex **4'**, the excitation energies are observed to undergo a large blue-shift in comparison to the trend from **1'** to **3'**. This is in line with the observed large blue-shift in the absorption profile of **4** in the experimental spectra and the observation that the LUMO of **4'** is dramatically destabilized relative to those of **1'**–**3'**. For complexes **2'** and **3'**, the lowest energy singlet excitations, S₁, appearing at 456 and 434 nm, respectively, correspond to HOMO → LUMO transitions and are therefore ¹MLCT in character. As with **1'**, these transitions contribute little to the absorption spectra due to having very small oscillator strengths. For **2'**, the first transitions of significance correspond to excitation to the S₅ and S₆ states at 406 and 389 nm, respectively, and are largely composed of transitions from HOMO – 1 and HOMO – 2 to the LUMO and LUMO + 1 orbitals. This confirms the assignment of the lower energy absorption bands in this region as arising from ¹MLCT with charge transfer to the bpy ligands.

For **3'**, the first major excitation, S₃, is similarly ¹MLCT in character (HOMO – 2 → LUMO) and again involves charge transfer to bpy rather than btz. Both **2'** and **3'** show ¹MLCT transitions in the region around 300–314 nm that involve excitation to orbitals with significant btz character. This therefore confirms

our assignment of the shoulders observed for **2** and **3** that appear in this region of their absorption spectra to ¹MLCT transitions with charge transfer to btz. These absorptions are also coincident with the lowest energy major band in the spectrum for **4**, and so would be consistent with this assignment.

We had reasoned that the observed quenching of the emission from the complexes on inclusion of the btz ligand may be in part due to the rise in energy of the ³MLCT state. The resultant proximity to the lowest ³MC state could then allow the thermal population of the latter, leading to non-radiative deactivation to the ground state. We would of course expect this to be most pronounced for **4**, based on spectroscopic data and the calculated orbital energies. The lowest energy singlet excited states that have significant ¹MC contributions are S₁₁ (343 nm, 1.01 eV above S₁) for **1'**, S₉ (344 nm, 0.89 eV above S₁) for **2'** and S₄ (360 nm, 0.59 eV above S₁) for **3'**. These transitions are all of low oscillator strength (>0.004) and therefore contribute little to the absorption spectrum. Nevertheless, replacement of bpy by btz and the consequent raising of the LUMO with respect to the δσ* orbitals does indeed result in a narrowing of the gap between the ¹MLCT and ¹MC states. For complex **4'** on the other hand, the lowest energy singlet excited state with an excitation at 340 nm is not of btz-centred ¹MLCT character but, to our surprise, is instead a ¹MC state corresponding to the excitation of an electron from the Ru 4d_{z²} orbital to the LUMO + 9 δσ* orbital. ¹MLCT transitions are instead observed to appear at 303–304 nm (S₁₀ and S₁₁) in the same region as the ¹MLCT transitions with significant btz character observed for **2'** and **3'**. Thus, replacement of the final bpy ligand results in a switching in the order of the lowest energy excited states from ¹MLCT in nature to ¹MC.

To further understand the photophysical properties of these complexes we proceeded to calculate the optimised geometries of the lowest lying triplet excited states using the constraint of a

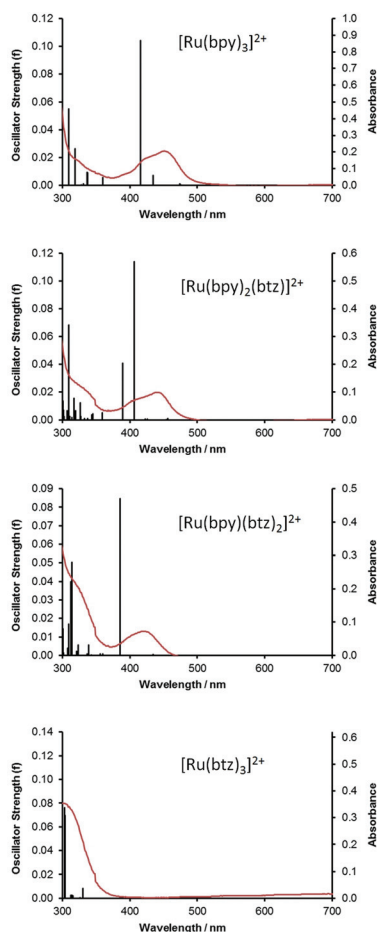


Fig. 5 TDDFT calculated absorption spectra for complexes $[\text{Ru}(\text{bpy})_{3-n}(\text{btz})_n]^{2+}$.

spin multiplicity of 3. The optimisation of the T_1 state of **1'** results in the slight shortening of the Ru–N bonds lengths to two of the bpy ligands from an average of 2.114 to 2.095 Å, consistent with the convergence toward C_2 symmetry observed in similar calculations by Alary and co-workers.⁵⁴ For the heteroleptic complex **2'**, the Ru–N bond lengths for the bpy ligands *trans* to btz are observed to shorten by 0.053 Å. Here, the Ru–N bonds to btz elongate from 2.127 to 2.153 Å. For **3'**, the Ru–N bonds to bpy again shorten upon optimisation of the T_1 state from 2.100 for S_0 to 2.035 Å.

For complexes **1'**–**3'**, the SOMOs are very similar in appearance to the HOMO and LUMO orbitals of the singlet ground state. This then confirms these triplet excited states as being $^3\text{MLCT}$ in character.

We reasoned that since the lowest lying singlet excited state for **4'** has ^1MC character, the lowest lying triplet excited state would also have ^3MC character. Indeed, when the geometry of the lowest energy triplet excited state of **4'** is allowed to optimise starting from the geometry of the singlet ground state, two mutually *trans* Ru–N bonds are observed to elongate to 2.53 Å. Thus, the formation of the lowest energy triplet excited state of **4'** involves dechelation of two ligands to yield $[\text{Ru}(\kappa^2\text{-btz})(\kappa^1\text{-btz})_2]^{2+}$ (Fig. 6). Alary *et al.* were able to arrive at similar geometries for the ^3MC states of **1'** and the analogous homoleptic 2,2'-bipyazyl (bpz) and 1,4,5,8-tetraazaphenanthrene (tap)

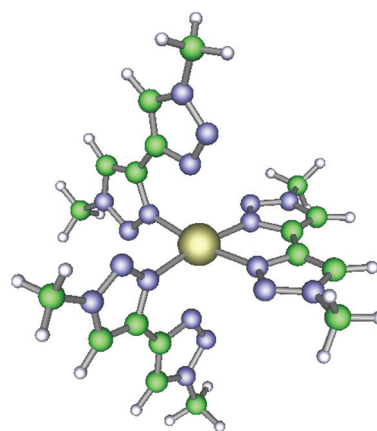


Fig. 6 Optimised geometry of the $^3\text{MC } T_1$ excited state of **4'**.

complexes, but through the use of appropriate Hartree–Fock initial guess vectors.^{54,55} Less pronounced elongation of the Ru–N bonds to 2.46 and 2.45 Å were observed for the ^3MC states of **1'** and $[\text{Ru}(\text{bpz})_3]^{2+}$ respectively but the corresponding Ru–N distances for $[\text{Ru}(\text{tap})_3]^{2+}$ (2.52 Å) are comparable to those found for **4'**. As a consequence of the structural deformation occurring during the optimisation of the T_1 state starting from the S_0 geometry of **4'**, the $d\sigma^*$ LUMO + 9 orbital for the ground state geometry undergoes a dramatic stabilisation and becomes the HOMO. Optimising the geometry of the S_0 state starting from this four-coordinate T_1 state results in the re-coordination of the two κ^1 -btz ligands and the restoration of the ground state geometry.

Whilst the DFT calculations presented here have been carried out in the gas phase and the calculated $^3\text{MLCT}$ states will therefore be stabilised through solvation, the photoexcitation of **4** may well proceed exclusively through this non-radiative photoreactive ^3MC state. This will therefore have an impact on the design of photoactive complexes and molecular devices that contain the btz ligand framework. Indeed, we have noticed that NMR samples of **3** in d_3 -MeCN that have been left to stand in daylight over two weeks appear to undergo conversion to at least one new complex along with the formation of a small amount of free ligand. At a much slower rate, **2** also converts into at least one new metal complex, again with a small amount of free btz formation. No discernable differences are observed in the spectra of **4** however. We are currently working to identify these new products and are probing the mechanism of formation to determine whether this is a thermal and/or photochemical process. Results from these further studies will be published in due course.

Conclusions

In conclusion, we have prepared and characterized complexes in the series $[\text{Ru}(\text{bpy})_{3-n}(\text{btz})_n]^{2+}$ ($n = 1$ to 3) and investigated the resultant photophysical effects of the btz ligand. The experimental data reveal a blue-shifting in the absorption bands consistent with the destabilization of the LUMO relative to the HOMO, with a larger blue-shift being observed on replacing the final bpy ligand by btz. The LUMO in all the bpy-containing complexes is bpy-centred, whereas that for **4** is btz-centred. The inclusion

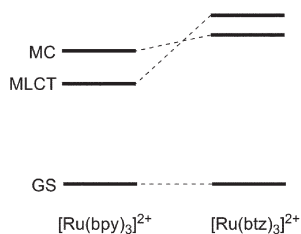


Fig. 7 Qualitative energy level diagram showing the change in the nature of the lowest energy excited states for $[\text{Ru}(\text{bpy})_3]^{2+}$ and $[\text{Ru}(\text{btzt})_3]^{2+}$ from MLCT to MC, respectively.

of btz also results in blue-shifted luminescent emission for $[\text{Ru}(\text{bpy})_2(\text{btzt})]^{2+}$, which is highly quenched compared to that of $[\text{Ru}(\text{bpy})_3]^{2+}$. Theoretical studies show that the lowest lying singlet and triplet excited states for all the bpy-containing complexes are MLCT in character, with the excited electron residing on the bpy ligands. The replacement of the final bpy ligand by btz in $[\text{Ru}(\text{btzt})_3]^{2+}$ results in a change in the nature of the lowest lying excited state from $^1\text{MLCT}$ to ^1MC (Fig. 7). The lowest lying triplet excited state is similarly ^3MC in nature and results in the dechelation of two btz ligands to yield $[\text{Ru}(\kappa^2\text{-btzt})(\kappa^1\text{-btzt})_2]^{2+}$. The excitation of this complex will therefore result in exclusive non-radiative deactivation to the ground state.

Experimental

General methods

$[\text{Ru}(\text{bpy})_3]\text{Cl}_2$, 2,2'-bipyridyl and 1,4-bis(trimethylsilyl)-1,3-butadiyne were purchased from Aldrich and used as supplied. $[\text{Ru}(p\text{-cymene})\text{Cl}_2]_2$ and $[\text{Ru}(p\text{-cymene})(\text{bpy})\text{Cl}]\text{PF}_6$ were prepared following the procedures in the literature.⁵⁶ NMR spectra were recorded on Bruker 500 Avance and 400 AMX spectrometers, UV-visible absorption spectra on a Varian Cary 300 spectrophotometer and luminescence spectra on a Hitachi F-4500 spectrophotometer. The 77 K emission spectra were recorded on a Jobin Yvon Fluoromax spectrometer. The samples were dissolved in acetonitrile and the spectra were recorded immediately. Mass spectra were collected on a Bruker Micro-Q-TOF instrument. Electrochemical measurements on the complexes were carried out at concentrations of 1 mM in 100 mM solutions of $\text{N}(\text{Bu})_4\text{PF}_6$ in acetonitrile. The data were referenced against $\text{Ag}-\text{AgCl}$ (3 M $\text{KCl}_{(\text{aq})}$) and all samples are quoted relative to ferrocene-ferrocenium. A glassy carbon electrode was used for the working electrode and a platinum counter electrode was used.

Synthesis of ligand and complexes

Synthesis of 1,1'-dibenzyl-4,4'-bi-1,2,3-triazolyl (btz). 1,4-bis(trimethylsilyl)-1,3-butadiyne (97 mg, 0.5 mmol), benzyl azide (133 mg, 1 mmol), $\text{CuSO}_4 \cdot 5\text{H}_2\text{O}$ (32 mg, 0.13 mmol), sodium ascorbate (79 mg, 0.4 mmol), K_2CO_3 (136 mg, 1 mmol) and pyridine (0.4 cm³, 5 mmol) were added to a flask containing 1 : 1 *tert*-butanol– H_2O (10 cm³). The mixture was stirred vigorously for 24 hours and then partitioned between dichloromethane and 5% aqueous ammonia. The organic layer was

separated and dried over MgSO_4 , filtered, and the solvent removed under reduced pressure to yield the product as a white solid. The characterisation data match those previously reported. Yield 111 mg, 70%.

^1H NMR (500 MHz) CD_3CN δ_{H} 5.62 (s, 4H, CH_2), 7.36–7.41 (m, 10H, Ph), 8.17 (s, 2H, CHN_3).

Synthesis of $[\text{Ru}(\text{bpy})_2(\text{btzt})][\text{PF}_6]_2$ (2). $[\text{Ru}(\text{bpy})_2\text{Cl}_2]$ (100 mg, 0.21 mmol) and btz (68 mg, 0.23 mmol) were suspended in ethanol (25 cm³) and refluxed under nitrogen for 4 hours. The solution was allowed to cool to room temperature, concentrated and passed through a silica column using $\text{MeCN}/\text{H}_2\text{O}/\text{sat}$ with $\text{KNO}_3(\text{aq})$ as the eluent. The orange band for the product was collected and reduced to dryness. The residues were dissolved in ethanol (10 cm³) and the product collected as an orange precipitate by addition of excess NH_4PF_6 . Yield 139 mg, 65%.

^1H NMR (500 MHz) CD_3CN δ_{H} 5.50 (d, $^2J_{\text{HH}} = 14.9$ Hz, 2H, CHH of Bz), 5.55 (d, $^2J_{\text{HH}} = 14.9$ Hz, 2H, CHH of Bz), 7.11–7.12 (m, 4H, *ortho*-Ph), 7.34–7.40 (m, 8H, *meta*- & *para*-Ph & $\text{H}_5\text{-bpy}$), 7.45 (ddd, $^4J_{\text{HH}} = 1.2$ Hz, $^3J_{\text{HH}} = 5.6$ Hz, $^3J_{\text{HH}} = 7.6$ Hz, 2H, $\text{H}_5\text{-bpy}$), 7.90 (at, $^3J_{\text{HH}} = 6.0$ Hz, 4H, $\text{H}_6\text{-bpy}$), 8.05 (td, $^4J_{\text{HH}} = 1.6$ Hz, $^3J_{\text{HH}} = ^3J_{\text{HH}} = 8.1$ Hz, 2H, H_4), 8.10 (td, $^4J_{\text{HH}} = 1.5$ Hz, $^3J_{\text{HH}} = ^3J_{\text{HH}} = 7.9$ Hz, 2H, H_4), 8.37 (s, 2H, CHN_3), 8.48 (at, $^3J_{\text{HH}} = 8.7$ Hz, 4H, $\text{H}_3\text{-bpy}$); ^{13}C NMR (125.8 MHz) CD_3CN δ_{C} 55.3 (CH_2), 123.4, 123.5, 123.8, 126.7, 127.4, 128.0, 128.9, 129.1 (all CH), 134.0 (C), 137.6 (CH), 140.4 (C), 137.7, 152.0, 152.4 (all CH), 157.3, 157.8 (all C).

HRMS (ESI) calcd for $\text{C}_{38}\text{H}_{32}\text{N}_{10}\text{Ru}$ 365.092197 (M^{2+}), found 365.092938.

Synthesis of $[\text{Ru}(\text{bpy})(\text{btzt})_2][\text{PF}_6]_2$ (3). $[\text{Ru}(p\text{-cymene})(\text{bpy})\text{Cl}]\text{PF}_6$ (50 mg, 0.082 mmol), btz (52 mg, 0.16 mmol) and NaPF_6 (60 mg, 0.18 mmol) were suspended in a 3 : 1 EtOH– H_2O mixture (8 cm³) under nitrogen and heated to 90 °C overnight. On cooling, a bright yellow–orange precipitate formed, which was isolated by filtration and washed with ether. The product was then recrystallized from dichloromethane–ether. Yield 69 mg, 71%.

^1H NMR (500 MHz) CD_3CN δ_{H} 5.49 (br s, 4H, CH_2 of Bz), 5.53 (s, 4H, CH_2 of Bz), 7.09–7.12 (m, 4H, Ph), 7.13–7.14 (m, 4H, Ph), 7.30–7.33 (m, 10H, Ph), 7.34–7.39 (m, 4H, Ph & $\text{H}_5\text{-bpy}$), 7.98 (ddd, $^5J_{\text{HH}} = 0.6$ Hz, $^4J_{\text{HH}} = 1.4$ Hz, $^3J_{\text{HH}} = 5.7$ Hz, 2H, $\text{H}_6\text{-bpy}$), 8.03 (td, $^4J_{\text{HH}} = 1.5$ Hz, $^3J_{\text{HH}} = ^3J_{\text{HH}} = 7.9$ Hz, 2H, $\text{H}_4\text{-bpy}$), 8.30 (s, 2H, CHN_3), 8.31 (s, 2H, CHN_3), 8.40 (dt, $^5J_{\text{HH}}$ & $^4J_{\text{HH}} = 1.0$ Hz, $^3J_{\text{HH}} = 8.7$ Hz, 2H, $\text{H}_3\text{-bpy}$).

HRMS (ESI) calcd for $\text{C}_{46}\text{H}_{40}\text{N}_{14}\text{Ru}$ (M^{2+}) 445.129645, found 445.131811.

Synthesis of $[\text{Ru}(p\text{-cymene})(\text{btzt})\text{Cl}]\text{PF}_6$. $[\text{Ru}(p\text{-cymene})\text{Cl}_2]_2$ (100 mg, 0.16 mmol) and btz (209 mg, 0.66 mmol) were suspended in methanol (10 cm³) and stirred for 3 hours. To the resultant yellow solution was added NH_4PF_6 (108 mg, excess) dissolved in methanol (1 cm³) and the volume of solution was reduced until the product precipitated as a bright yellow powder. The product was collected by filtration, washed with ether and air dried. Yield 205 mg, 88%.

^1H NMR (500 MHz) CD_3CN δ_{H} 1.07 (s, 3H, $\text{CH}(\text{CH}_3)$), 1.09 (s, 3H, $\text{CH}(\text{CH}_3)$), 2.15 (s, 3H, CH_3), 2.73 (sp, $^3J_{\text{HH}} = 6.9$ Hz, 1H, $\text{CH}(\text{CH}_3)_2$), 5.64 (d, $^3J_{\text{HH}} = 6.3$ Hz, 2H, *p*-cymene), 5.70 (d,

$^2J_{\text{HH}} = 14.9$ Hz, 2H, CHH of Bz), 5.76 (d, $^2J_{\text{HH}} = 14.9$ Hz, 2H, CHH of Bz), 5.85 (d, $^3J_{\text{HH}} = 6.3$ Hz, 2H, *p*-cymene), 7.38–7.45 (m, 10H, Ph), 8.27 (s, 2H, CHN₃); ^{13}C NMR (125.8 MHz) CD₃CN δ_{C} 17.8 (CH₃, *p*-cymene), 21.3 (CH₃, CH(CH₃)₂), 30.7 (CH, CH(CH₃)₂), 55.8 (CH₂), 83.0 (CH, *p*-cymene), 85.2 (CH, *p*-cymene), 101.6 (C, *p*-cymene), 104.6 (C, *p*-cymene), 122.8, 128.5, 129.1, 129.2 (all CH, btz), 134.0, 138.5 (C, btz).

HRMS (ESI) calcd for C₂₈H₃₀NCIRu (M⁺) 587.12549, found 587.126586.

Synthesis of [Ru(btz)₃][PF₆]₂ (4). [Ru(*p*-cymene)(btz)Cl]PF₆ (50 mg, 0.068 mmol), btz (44 mg, 0.14 mmol) and NaPF₆ (66 mg, 0.39 mmol) were suspended in a 3 : 1 EtOH–H₂O mixture (8 cm³) under nitrogen and heated to 90 °C overnight. On cooling, a pale yellow precipitate formed, which was isolated by filtration and washed with ether. The product was then recrystallized from dichloromethane–ether as a pale tan solid. Yield 71 mg, 78%.

^1H NMR (500 MHz) CD₃CN δ_{H} 5.52 (s, 12H, CH₂), 7.11–7.13 (m, 12H, Ph), 7.28–7.35 (m, 18H, Ph), 8.34 (s, 6H, CHN₃); ^{13}C NMR (125.8 MHz) CD₃CN δ_{C} 55.2 (CH₂), 122.7, 127.8, 128.9, 129.1 (all CH), 134.3, 141.0 (all C).

HRMS (ESI) calcd for C₅₄H₄₈N₁₈Ru (M²⁺) 525.167093, found 525.169291.

Computational details

DFT calculations were carried out using the GAMESS-UK⁵⁷ and NWChem⁵⁸ software packages. Calculations were carried out using the B3LYP hybrid functional (20% Hartree–Fock),⁵⁹ Stuttgart relativistic small core ECP for ruthenium⁶⁰ and 6-311G* basis sets for all other atoms.⁶¹ Molecular structures and molecular orbitals were visualized using the ccp1 graphical user interface. The ground state geometries of all complexes were first optimized and molecular orbital energies determined. TDDFT calculations were then used at the ground state geometries to derive the vertical excitation energies and hence the simulated absorption spectra. The geometries of the lowest lying triplet states were optimised starting from the geometries of the ground states using the constraint of a spin multiplicity of 3.

X-Ray crystallography

Single crystal X-ray diffraction data were collected on a Bruker Apex Duo diffractometer equipped with a graphite monochromated Mo(K α) radiation source (0.071073 nm) and a cold stream of N₂ gas. Summarised crystal and refinement data are presented in Table 4. Preliminary scans were employed to assess the crystal quality, lattice symmetry, ideal exposure time, *etc.*, prior to collecting a full sphere of diffraction intensity data using the SMART operating software.⁶² Intensities were then integrated from several series of exposures, merged and corrected for Lorentz and polarisation effects using the SAINT software.⁶³ Solutions were generated by conventional heavy atom Patterson or direct methods and refined by full-matrix non-linear least squares on all F^2 data, using the SHELXS-97 and SHELXL software, respectively (as implemented in the SHELXTL suite of programs).⁶⁴ Empirical absorption corrections were applied based on multiple and symmetry-equivalent measurements using

Table 4 X-Ray crystallographic data for [Ru(bpy)₂(btz)][PF₆]₂·2 MeCN

Formula	C ₄₂ H ₃₈ F ₁₂ N ₁₂ P ₂ Ru
$M_r/\text{g mol}^{-1}$	1101.85
Temperature/K	150
Space group	Pbcn
$a/\text{\AA}$	17.4573(7)
$b/\text{\AA}$	15.6748(6)
$c/\text{\AA}$	16.6134(6)
$\alpha/^\circ$	90
$\beta/^\circ$	90
$\gamma/^\circ$	90
$V/\text{\AA}^3$	4546.1(3)
$D_c/\text{g cm}^{-3}$	1.610
Z	4
$\mu_{\text{Mo}}/\text{mm}^{-1}$	0.512
$T_{\text{min, max}}$	0.790, 0.880
$2\theta_{\text{max}}$	64.06
N_{ref}	7884
R_1	0.0452
wR_2	0.1445
S	0.977

SADABS.⁶⁵ All structures were refined until convergence (max shift/esd < 0.01) and in each case, the final Fourier difference map showed no chemically sensible features.

Acknowledgements

The authors thank the University of Huddersfield and the Leverhulme Trust for funding this research. We also thank the Huddersfield Centre for High Performance Computing, the National Grid Service and Science and Technology Facilities Council (Daresbury Laboratories) for computational resources and support. We also thank Dr Daniel Sykes (University of Sheffield) for technical assistance.

Notes and references

- V. V. Rostovtsev, L. G. Green, V. V. Fokin and K. B. Sharpless, *Angew. Chem., Int. Ed.*, 2002, **41**, 2596.
- M. Meldal and C. W. Tomoe, *Chem. Rev.*, 2008, **108**, 2952.
- D. Fournier, R. Hoogenboom and U. S. Schubert, *Chem. Soc. Rev.*, 2007, **36**, 1369–1380.
- G. Franc and A. K. Kakkar, *Chem. Soc. Rev.*, 2010, **39**, 1536–1544.
- P. L. Golas and K. Matyjaszewski, *Chem. Soc. Rev.*, 2010, **39**, 1338–1354.
- J. C. Jewett and C. R. Bertozzi, *Chem. Soc. Rev.*, 2010, **39**, 1272–1279.
- K. Kempe, A. Krieg, C. R. Becer and U. S. Schubert, *Chem. Soc. Rev.*, 2012, **41**, 176–191.
- A. H. El-Sagheer and T. Brown, *Chem. Soc. Rev.*, 2010, **39**, 1388–1405.
- J. A. Prescher and C. R. Bertozzi, *Nat. Chem. Biol.*, 2005, **1**, 13.
- E. Amadio, M. Bertoldini, A. Scrivanti, G. Chessa, V. Beghetto, U. Matteoli, R. Bertani and A. Dolmella, *Inorg. Chim. Acta*, 2011, **370**, 388–393.
- S. Bedeche, J.-C. Daran, J. Ruiz and D. Astruc, *Inorg. Chem.*, 2008, **47**, 4903.
- B. Beyer, C. Ulbricht, D. Escudero, C. Friebe, A. Winter, L. Gonzalez and U. S. Schubert, *Organometallics*, 2009, **28**, 5478.
- B. Beyer, C. Ulbricht, A. Winter, M. D. Hager, R. Hoogenboom, N. Herzer, S. O. Baumann, G. Kickelbick, H. Gorgs and U. S. Schubert, *New J. Chem.*, 2010, **34**, 2622.
- I. Bratsos, D. Urankar, E. Zangrando, P. Genova-Kalou, J. Kosmrlj, E. Alessio and I. Turel, *Dalton Trans.*, 2011, **40**, 5188–5199.
- J. D. Crowley and P. H. Bandeen, *Dalton Trans.*, 2010, **39**, 612.
- J. D. Crowley, P. H. Bandeen and L. R. Hanton, *Polyhedron*, 2010, **29**, 70–83.

- 17 J. M. Fernandez-Hernandez, C.-H. Yang, J. I. Beltran, V. Lemaire, F. Polo, R. Frohlich, J. Cornil and L. De Cola, *J. Am. Chem. Soc.*, 2011, **133**, 10543.
- 18 O. Fleischel, N. Wu and A. Petitjean, *Chem. Commun.*, 2010, **46**, 8454.
- 19 M. L. Gower and J. D. Crowley, *Dalton Trans.*, 2010, **39**, 2371–2378.
- 20 G. Guisado-Barrios, J. Bouffard, B. Donnadiou and G. Bertrand, *Organometallics*, 2011, **30**, 6017.
- 21 M. Juriceck, M. Felici, P. Contreras-Carballada, J. Lauko, S. R. Bou, P. H. J. Kouwer, A. M. Brouwer and A. E. Rowan, *J. Mater. Chem.*, 2011, **21**, 2104.
- 22 K. J. Kilpin and J. D. Crowley, *Polyhedron*, 2010, **29**, 3111–3117.
- 23 K. J. Kilpin, E. L. Gavey, C. J. McAdam, C. B. Anderson, S. J. Lind, C. C. Keep, K. C. Gordon and J. D. Crowley, *Inorg. Chem.*, 2011, **50**, 6334–6346.
- 24 S. Ladouceur, D. Fortin and E. Zysman-Colman, *Inorg. Chem.*, 2011, **50**, 11514.
- 25 R. Lalrempuia, N. D. McDaniel, H. Muller-Bunz, S. Bernhard and M. Albrecht, *Angew. Chem., Int. Ed.*, 2010, **49**, 9765.
- 26 L. Liang and D. Astruc, *Coord. Chem. Rev.*, 2011, **255**, 2933–2945.
- 27 S. Liu, P. Muller, M. K. Takase and T. M. Swager, *Inorg. Chem.*, 2011, **50**, 7598.
- 28 P. Mathew, A. Neels and M. Albrecht, *J. Am. Chem. Soc.*, 2008, **130**, 13534.
- 29 H. A. Michaels, C. S. Murphy, R. J. Clark, M. W. Davidson and L. Zhu, *Inorg. Chem.*, 2010, **49**, 4278–4287.
- 30 T. Romero, R. A. Orenes, A. Espinosa, A. Tarraga and P. Molina, *Inorg. Chem.*, 2011, **50**, 8214.
- 31 B. Schulze, D. Escudero, C. Friebe, R. Siebert, H. Goerls, U. Kohn, E. Altuntas, A. Baumgaertel, M. D. Hager, A. Winter, B. Dietzek, J. Popp, L. Gonzalez and U. S. Schubert, *Chem.–Eur. J.*, 2011, **17**, 5494.
- 32 B. Schulze, C. Friebe, M. D. Hager, A. Winter, R. Hoogenboom, H. Goerls and U. S. Schubert, *Dalton Trans.*, 2009, 787–794.
- 33 E. M. Schuster, M. Botoshansky and M. Gandelman, *Organometallics*, 2009, **28**, 7001–7005.
- 34 D. Schweinfurth, S. Strobel and B. Sarkar, *Inorg. Chim. Acta*, 2011, **374**, 253–260.
- 35 E. A. S. Smith, G. Molev, M. Botoshansky and M. Gandelman, *Chem. Commun.*, 2011, **47**, 319–321.
- 36 For recent reviews of the area, see: H. Struthers, T. L. Mindt and R. Schibli, *Dalton Trans.*, 2010, **39**, 675–696; J. D. Crowley and D. A. McMorran, *Top. Heterocyclic Chem.*, 2012, DOI: 10.1007/7081_2011-67.
- 37 Y. Tulchinsky, M. A. Iron, M. Botoshansky and M. Gandelman, *Nat. Chem.*, 2011, **3**, 525–531.
- 38 L. Wang, W.-W. Yang, R.-H. Zheng, Q. Shi, Y.-W. Zhong and J. Yao, *Inorg. Chem.*, 2011, **50**, 7074.
- 39 W.-W. Yang, Y.-W. Zhong and J. Yao, *Organometallics*, 2011, **30**, 2236.
- 40 M. Obata, A. Kitamura, A. Mori, C. Kameyama, J. A. Czaplewski, R. Tanaka, I. Kinoshita, T. Kusumoto, H. Hashimoto, M. Harada, Y. Mikata, T. Funabiki and S. Yano, *Dalton Trans.*, 2008, 3292–3300.
- 41 M. Felici, P. Contreras-Carballada, Y. Vida, J. M. M. Smits, R. J. M. Nolte, L. De Cola, R. M. Williams and M. C. Feiters, *Chem.–Eur. J.*, 2009, **15**, 13124–13134.
- 42 M. Mydlak, C. Bizzarri, D. Hartmann, W. Sarfet, G. Schmid and L. De Cola, *Adv. Funct. Mater.*, 2010, **20**, 1812.
- 43 E. Orselli, R. Q. Albuquerque, P. M. Fransen, R. Frohlich, H. M. Janssen and L. De Cola, *J. Mater. Chem.*, 2008, **18**, 4579.
- 44 S. Zanarini, M. Felici, G. Valenti, M. Maracaccio, L. Prodi, S. Bonacchi, P. Contreras-Carballada, R. M. Williams, M. C. Feiters, R. J. M. Nolte, L. De Cola and F. Paolucci, *Chem.–Eur. J.*, 2011, **17**, 4640.
- 45 B. Happ, D. Escudero, M. D. Hager, C. Friebe, A. Winter, H. Goerls, E. Altuntas, L. Gonzalez and U. S. Schubert, *J. Org. Chem.*, 2010, **75**, 4025–4038.
- 46 B. Happ, C. Friebe, A. Winter, M. D. Hager, R. Hoogenboom and U. S. Schubert, *Chem.–Asian J.*, 2009, **4**, 154–163.
- 47 I. Stengel, A. Mishra, N. Pootrakulchote, S.-J. Moon, S. M. Zakeeruddin, M. Graetzel and P. Bauerle, *J. Mater. Chem.*, 2011, **21**, 3726–3734.
- 48 B. Durham, J. V. Caspar, J. K. Nagle and T. J. Meyer, *J. Am. Chem. Soc.*, 1982, **104**, 4803–4810.
- 49 A. Juris, V. Balzani, F. Barigelletti, S. Campagna, P. Belser and A. Vonzelewsky, *Coord. Chem. Rev.*, 1988, **84**, 85–277.
- 50 J. Vanhouten and R. J. Watts, *J. Am. Chem. Soc.*, 1976, **98**, 4853–4858.
- 51 J. T. Fletcher, B. J. Bumgarner, N. D. Engels and D. A. Skoglund, *Organometallics*, 2008, **27**, 5430–5433.
- 52 U. Monkowius, S. Ritter, B. Konig, M. Zabel and H. Yersin, *Eur. J. Inorg. Chem.*, 2007, 4597–4606.
- 53 A. Mattiuzzi, I. Jabin, C. Moucheron and A. Kirsch-De Mesmaeker, *Dalton Trans.*, 2011, **40**, 7395–7402.
- 54 F. Alary, M. Boggio-Pasqua, J.-L. Heully, C. J. Marsden and P. Vicendo, *Inorg. Chem.*, 2008, **47**, 5259–5266.
- 55 F. Alary, J. L. Heully, L. Bijeire and P. Vicendo, *Inorg. Chem.*, 2007, **46**, 3154–3165.
- 56 M. A. Bennett, T.-N. Huang, T. W. Matheson and A. K. Smith, *Inorg. Synth.*, 1982, **21**, 74.
- 57 M. F. Guest, I. J. Bush, H. J. J. van Dam, P. Sherwood, J. M. H. Thomas, J. H. van Lenthe, R. W. A. Havenith and J. Kendrick, *Mol. Phys.*, 2005, **103**, 719.
- 58 M. Valiev, E. J. Bylaska, N. Govind, K. Kowalski, T. P. Straatsma, H. J. J. van Dam, D. Wang, J. Nieplocha, E. Apra, T. L. Windus and W. A. de Jong, *Comput. Phys. Commun.*, 2010, **181**, 1477.
- 59 P. J. Stephens, F. J. Devlin, C. F. Chabalowski and M. J. Frisch, *J. Phys. Chem.*, 1994, **98**, 11623–11627.
- 60 D. Andrae, U. Haussermann, M. Dolg, H. Stoll and H. Preuss, *Theor. Chim. Acta*, 1990, **77**, 123–141.
- 61 R. Krishnan, J. S. Binkley, R. Seeger and J. A. Pople, *J. Chem. Phys.*, 1980, **72**, 650–654.
- 62 *SMART Diffractometer Control Software*, Bruker Analytical X-ray Instruments Inc., Madison, WI, 1998.
- 63 *SAINT Integration Software*, Siemens Analytical X-ray Instruments Inc., Madison, WI, 1994.
- 64 *SHELXTL Program System, Vers 5.1*, Bruker Analytical X-ray Instruments Inc., Madison, WI, 1998.
- 65 G. M. Sheldrick, *SADABS: A Program for Absorption Correction with Siemens SMART System*, University of Gottingen, Germany, 1996.